

Control Synthesis of Cyber-Physical Systems for Real-Time Specifications through Causation-Guided Reinforcement Learning

Xiaochen Tang[✉]

School of Computer Science and Technology,
Tongji University
Shanghai, China
xiaochen9697@tongji.edu.cn

Zhenya Zhang^{*✉}

Faculty of Information Science and Electrical Engineering,
Kyushu University, Fukuoka, Japan
& National Institute of Informatics, Tokyo, Japan
zhang@ait.kyushu-u.ac.jp

Miaomiao Zhang^{*✉}

School of Computer Science and Technology,
Tongji University
Shanghai, China
miaomiao@tongji.edu.cn

Jie An^{*✉}

National Key Lab. of Space Integrated Information System,
Institute of Software, Chinese Academy of Sciences,
Beijing, China
anjie@iscas.ac.cn

Abstract—In real-time and safety-critical cyber-physical systems (CPSs), control synthesis must guarantee that generated policies meet stringent timing and correctness requirements under uncertain and dynamic conditions. Signal temporal logic (STL) has emerged as a powerful formalism of expressing real-time constraints, with its semantics enabling quantitative assessment of system behavior. Meanwhile, reinforcement learning (RL) has become an important method for solving control synthesis problems in unknown environments. Recent studies incorporate STL-based reward functions into RL to automatically synthesize control policies. However, the automatically inferred rewards obtained by these methods represent the global assessment of a whole or partial path but do not accumulate the rewards of local changes accurately, so the sparse global rewards may lead to non-convergence and unstable training performances. In this paper, we propose an online reward generation method guided by the online causation monitoring of STL. Our approach continuously monitors system behavior against an STL specification at each control step, computing the quantitative distance toward satisfaction or violation and thereby producing rewards that reflect instantaneous state dynamics. Additionally, we provide a smooth approximation of the causation semantics to overcome the discontinuity of the causation semantics and make it differentiable for using deep-RL methods. We have implemented a prototype tool and evaluated it in the Gym environment on a variety of continuously controlled benchmarks. Experimental results show that our proposed STL-guided RL method with online causation semantics outperforms existing relevant STL-guided RL methods, providing a more robust and efficient reward generation framework for deep-RL.

Index Terms—control synthesis, CPS, STL, real-time specification, reinforcement learning

I. INTRODUCTION

Cyber-physical systems (CPSs) [1], [2] are assigned increasingly complex objectives including reactive and sequential

tasks in domains such as autonomous vehicles, advanced manufacturing, and health care systems. *Temporal logics* [3] are widely adopted to specify properties and verify behaviors of CPSs due to their rich and rigorous expressiveness. However, some tasks in the CPS have not only temporal requirements, but also more stringent deadline constraints. *Signal Temporal Logic* (STL) [4]–[6] introduces real-time intervals and continuous signal predicates to precisely express real-time constraints such as “respond in $[a, b]$ time” and “continuously satisfy safety conditions”. The *robust semantics* [4] of STL provides quantitative satisfaction measures that allow the system to assess the extent to which trajectories satisfy or violate the specification, while STL-based online monitors enable real-time monitoring and alerting of CPS. In addition, the use of STL to guide the automatic synthesis of controllers has attracted research attention in CPS areas such as robotics [7] and transportation network control [8]. Typical approaches are translating STL specifications into mixed-integer linear constraints and embedding them into model predictive control (MPC) frameworks [9], [10], and converting STL formulas into finite automata for automata-guided path planning [11]–[13]. However, it is a great challenge to establish a reliable mathematical model due to the complex dynamics of the system and the intricate design objectives involved.

Model-free *reinforcement learning* (RL) [14] has emerged as an effective method to address complex control synthesis problems of CPSs with unknown environment dynamics. Recent works [15] incorporate STL semantics into RL to generate rewards for complex RL tasks. The powerful expressiveness of STL makes it effectively express complex control objectives in RL, which are difficult to achieve with a handcrafted reward function. Moreover, the robust semantics of STL provides a quantitative way to show how much a trajectory satisfies

* Corresponding authors.

or violates a system specification, which can significantly improve the stability and performance of control policy synthesis in complex CPS tasks using RL. Nevertheless, reward functions based on STL robust semantics are global, i.e., the rewards are only available over an entire episode, which will affect all states in a learning episode. These non-Markovian reward functions may lead to non-convergence and unstable training performances. To mitigate the problem, within the deep-RL framework [16], Balakrishnan and Deshmukh [17] utilized the robustness value of a partial signal as the reward of its last state. Therefore, in each step, the reward of the current state can be computed based on the robustness value of the corresponding partial signal. Following the idea, Singh and Saha [18] proposed a new aggregation-based smooth approximation of STL semantics of partial signals additionally, making it more friendly to the existing deep-RL algorithms.

However, these STL-guided RL methods with single states as network inputs still suffer from the problem of non-Markovianity, since the reward functions are based on a partial sequence of states. In addition, based on the robust semantics, it is difficult to solve the problem intrinsically, since the robust semantics of STL may not accurately describe the system's evolution at the current instant [19], [20]. Recently, *online causation semantics* [21] is proposed as an alternative of online robust semantics [22] and provides more detailed information on changes of system states than the robust semantics. Unlike classic online robust monitoring approaches that aim to measure *whether or not* a partial signal violates the given specification, causation semantics considers whether each instant can be treated as the *causation* of the violation, thus offering a refined assessment of each system state against the specification. This feature of causation semantics coincidentally matches the spirit of RL rewards in control synthesis, which also aim to give a precise assessment for each system state, and therefore, this motivates us to explore the assignment of RL rewards based on causation semantics.

In this paper, we propose a novel online causation-guided RL method for control synthesis of real-time systems. The main contributions of this paper are as follows.

- We applied the online causation monitor of STL to generate rewards for RL. The technical adjustments performed to make the online causation monitor suitable for RL involve:
 - . τ -MDP [15] is adopted to accommodate non-Markovianity;
 - . Sampling windows are proposed to avoid dealing with long trajectories that can diminish efficiency in RL;
 - . Smoothing approximation of the online causation semantics to meet the differentiable requirement of deep-RL.
- We have implemented a prototype and evaluated it on several challenging continuous control benchmarks available in the Gym environment [23].

We compare our method with the baseline RL method using hand-crafted reward functions and the existing STL-guided

RL method using the robust semantics. Experimental results demonstrate that our method converges more stably than other methods, and the trained control policies achieve higher values on three evaluation metrics.

II. PRELIMINARIES

A. Signal Temporal Logic

STL is a widely adopted formal language that can describe the real-time properties of a system. Let $T \in \mathbb{R}_+$ be a positive real, and $d \in \mathbb{N}_+$ be a positive integer. A d -dimensional signal is a function $\mathbf{v} : [0, T] \rightarrow \mathbb{R}^d$, where T is called the time *horizon* of \mathbf{v} . Given an arbitrary time instant $t \in [0, T]$, $\mathbf{v}(t)$ is a d -dimensional real vector, each dimension concerning a signal variable that has a certain physical meaning. In this paper, we fix a set \mathbf{Var} of variables and assume that a signal \mathbf{v} is spatially bounded, i.e., for all $t \in [0, T]$, $\mathbf{v}(t) \in \Omega$, where Ω is a d -dimensional hyper-rectangle. The syntax of STL is defined as follows.

Definition 1 (STL syntax): In STL, the atomic propositions α and the formulas φ are defined as follows:

$$\begin{aligned} \alpha &::= f(x_1, \dots, x_K) > 0 \\ \varphi &::= \alpha \mid \top \mid \neg\varphi \mid \varphi_1 \wedge \varphi_2 \mid \square_I\varphi \mid \diamond_I\varphi \mid \varphi_1 \mathcal{U}_I\varphi_2 \end{aligned} \quad (1)$$

where \top means *true*, f is a K -ary function $f : \mathbb{R}^K \rightarrow \mathbb{R}$, $x_1, \dots, x_K \in \mathbf{Var}$, and I is a closed interval over \mathbb{R}_+ , i.e., $I = [l, u]$, where $l, u \in \mathbb{R}_+$ and $l \leq u$. The operators \neg and \wedge denote logical NOT and AND operators. Other logical operators like logical OR (\vee) and implication (\Rightarrow) can be derived using \neg and \wedge , where $\varphi_1 \vee \varphi_2 \equiv \neg(\neg\varphi_1 \wedge \neg\varphi_2)$ and $\varphi_1 \Rightarrow \varphi_2 \equiv \neg\varphi_1 \vee \varphi_2$. The temporal operator \mathcal{U}_I is the Until operator implying that φ_2 becomes true sometime in the time interval I and φ_1 must remain true until φ_2 becomes true. The other two temporal operators are known as Eventually (\diamond_I) and Always (\square_I), where $\diamond_I\varphi \equiv \top \mathcal{U}_I\varphi$ and $\square_I\varphi \equiv \neg\diamond_I\neg\varphi$.

Definition 2 (STL robust semantics): Let \mathbf{v} be a signal, φ be an STL formula and $\mu \in \mathbb{R}_+$ be an instant. The *robustness* $\rho(\mathbf{v}, \varphi, \mu) \in \mathbb{R} \cup \{\infty, -\infty\}$ of \mathbf{v} w.r.t. φ at μ is defined by induction on the construction of formulas, as:

$$\begin{aligned} \rho(\mathbf{v}, \alpha, \mu) &:= f(\mathbf{v}(\mu)), \\ \rho(\mathbf{v}, \top, \mu) &:= \infty, \\ \rho(\mathbf{v}, \neg\varphi, \mu) &:= -\rho(\mathbf{v}, \varphi, \mu), \\ \rho(\mathbf{v}, \varphi_1 \wedge \varphi_2, \mu) &:= \min(\rho(\mathbf{v}, \varphi_1, \mu), \rho(\mathbf{v}, \varphi_2, \mu)), \\ \rho(\mathbf{v}, \square_I\varphi, \mu) &:= \inf_{t \in \mu+I} \rho(\mathbf{v}, \varphi, t), \\ \rho(\mathbf{v}, \diamond_I\varphi, \mu) &:= \sup_{t \in \mu+I} \rho(\mathbf{v}, \varphi, t), \\ \rho(\mathbf{v}, \varphi_1 \mathcal{U}_I\varphi_2, \mu) &:= \sup_{t \in \mu+I} \min(\rho(\mathbf{v}, \varphi_2, t), \inf_{t' \in [\mu, t]} \rho(\mathbf{v}, \varphi_1, t')). \end{aligned}$$

Here, $\mu + I$ denotes the interval $[l + \mu, u + \mu]$.

The robustness of a signal \mathbf{v} w.r.t a specification φ is defined as $\rho(\mathbf{v}, \varphi) = \rho(\mathbf{v}, \varphi, 0)$, i.e., the robustness at time 0. The original STL semantics is Boolean, which represents whether a signal \mathbf{v} satisfies φ at an instant μ , i.e., $(\mathbf{v}, \mu) \models \varphi$. The robust semantics in Definition 2 is a quantitative extension

that refines the original Boolean STL semantics, in the sense that, $\rho(\mathbf{v}, \varphi, \mu) > 0$ implies $(\mathbf{v}, \mu) \models \varphi$ and $\rho(\mathbf{v}, \varphi, \mu) < 0$ implies $(\mathbf{v}, \mu) \not\models \varphi$. Intuitively, it quantifies how strongly a given signal \mathbf{v} satisfies or violates a given formula φ .

For some discrete systems, control synthesis with STL specifications is decidable and tractable. For example, [9] formulates the STL control synthesis problem as a mixed integer linear program. However, in general, especially for complex continuous systems, the STL control problem is undecidable or computationally intractable.

B. Online Robust Semantics of STL

STL robust semantics in Definition 2 provide an offline monitoring approach for *complete signals*. *Online monitoring*, instead, targets a growing *partial signal* at runtime. The formal definitions of partial signals and the online robust semantics of STL are as follows.

For a signal \mathbf{v} with the time horizon T , let $[a, b] \subseteq [0, T]$ be a sub-interval in the time domain $[0, T]$. A *partial signal* $\mathbf{v}_{a:b}$ is a function which is only defined in the interval $[a, b]$; in the remaining domain $[0, T] \setminus [a, b]$, we denote the value of $\mathbf{v}_{a:b}$ at those instants as ϵ , where ϵ stands for a value that is not defined. Specifically, if $a = 0$ and $b \in (a, T]$, a partial signal $\mathbf{v}_{a:b}$ is called a *prefix* (partial) signal; dually, if $b = T$ and $a \in [0, b)$, a partial signal $\mathbf{v}_{a:b}$ is called a *suffix* (partial) signal. Given a prefix signal $\mathbf{v}_{0:b}$, a *completion* $\mathbf{v}_{0:b} \cdot \mathbf{v}_{b:T}$ of $\mathbf{v}_{0:b}$ is defined as the concatenation of $\mathbf{v}_{0:b}$ with a suffix signal $\mathbf{v}_{b:T}$.

Definition 3 (Online STL robust semantics): Let $\mathbf{v}_{0:b}$ be a prefix signal, and let φ be an STL formula. We denote by R_{\max}^{α} and R_{\min}^{α} the possible *maximum* and *minimum bounds* of the robustness $\rho(\mathbf{v}, \alpha, \mu)$ ¹. Then, an online robust semantics $[R](\mathbf{v}_{0:b}, \varphi, \mu)$, which returns a sub-interval of $[R_{\min}^{\alpha}, R_{\max}^{\alpha}]$ at the instant b , is defined as follows, by induction on the construction of formulas.

$$\begin{aligned} [R](\mathbf{v}_{0:b}, \alpha, \mu) &:= \begin{cases} [f(\mathbf{v}_{0:b}(\mu)), f(\mathbf{v}_{0:b}(\mu))] & \text{if } \mu \in [0, b] \\ [R_{\min}^{\alpha}, R_{\max}^{\alpha}] & \text{otherwise} \end{cases} \\ [R](\mathbf{v}_{0:b}, \neg\varphi, \mu) &:= -[R](\mathbf{v}_{0:b}, \varphi, \mu) \\ [R](\mathbf{v}_{0:b}, \varphi_1 \wedge \varphi_2, \mu) &:= \\ &\quad \min\left([R](\mathbf{v}_{0:b}, \varphi_1, \mu), [R](\mathbf{v}_{0:b}, \varphi_2, \mu)\right) \\ [R](\mathbf{v}_{0:b}, \Box_I \varphi, \mu) &:= \inf_{t \in \mu+I} \left([R](\mathbf{v}_{0:b}, \varphi, t)\right) \\ [R](\mathbf{v}_{0:b}, \varphi_1 \mathcal{U}_I \varphi_2, \mu) &:= \\ &\quad \sup_{t \in \mu+I} \min\left([R](\mathbf{v}_{0:b}, \varphi_2, t), \inf_{t' \in [\mu, t]} [R](\mathbf{v}_{0:b}, \varphi_1, t')\right) \end{aligned}$$

Here, f is defined as in Definition 1, and the arithmetic rules over intervals $I = [l, u]$ are defined as follows: $-I := [-u, -l]$ and $\min(I_1, I_2) := [\min(l_1, l_2), \min(u_1, u_2)]$.

We denote $[R]^U(\mathbf{v}_{0:b}, \varphi, \mu)$ and $[R]^L(\mathbf{v}_{0:b}, \varphi, \mu)$ as the upper bound and the lower bound of $[R](\mathbf{v}_{0:b}, \varphi, \mu)$ respectively.

¹ $\rho(\mathbf{v}, \alpha, \mu)$ is bounded because \mathbf{v} is bounded by Ω . In practice, if Ω is not known, we set R_{\max}^{α} and R_{\min}^{α} to, respectively, ∞ and $-\infty$.

Intuitively, the two bounds together form the reachable robustness interval of the completion $\mathbf{v}_{0:b} \cdot \mathbf{v}_{b:T}$, under any possible suffix signal $\mathbf{v}_{b:T}$.

C. Markov Decision Processes

A *Markov decision process (MDP)* [24] is a transition system in which state transitions take place non-deterministically following a probability distribution.

Definition 4 (MDP): An MDP is a tuple $\mathcal{M} = \langle S, A, P, R \rangle$, where

- S is a set of states and denotes the state-space,
- A is a finite set of input actions,
- $P : S \times A \times S \rightarrow [0, 1]$ is the probabilistic transition function where $P(s, a, s')$ denotes the probability of the transition from state s to s' by action a ,
- $R : S \rightarrow \mathbb{R}$ is a real-valued reward function.

A sequence of states is called a *trajectory*. For any integer $i, j \in \mathbb{N}_{\geq 0}$, let $s_i \in S$ denote the i -th state of an arbitrary trajectory in system (s_0 is the initial state), and $s_{i:j}$ denote the partial trajectory from the i -th state to the j -th state. Note that $s_{i:i} = s_i$. Let ω denote a finite-state trajectory, $\omega(i)$ denote the i -th element of ω , $\omega(-1)$ denote the last element of ω , and $\omega(i, j)$ denote the sub-trajectory of ω from the i -th element to the j -th element. A *policy* $\pi : S \rightarrow \text{Dist}(A)$ for a system \mathcal{M} is a function that maps each state to a distribution over the actions.

A policy π on \mathcal{M} can induce a *discrete-time Markov chain (DTMC)* $\mathcal{D}_{\mathcal{M}}^{\pi} = \langle \bar{S}, \bar{P} \rangle$, where $\bar{S} = S$ is a set of states and $\bar{P} : \bar{S} \rightarrow \text{Dist}(\bar{S})$ is a probabilistic transition function that maps a current state to a distribution over the next states, and $\bar{P}(\bar{s}, \bar{s}') = \sum_{a \in A} \pi(a|\bar{s})P(\bar{s}, a, \bar{s}')$ for any $\bar{s}, \bar{s}' \in \bar{S}$.

D. STL-Guided RL Methods

In control policy synthesis problems for complex CPSs with unknown models, STL-guided RL methods model the system models as MDPs, specify the system tasks in terms of STL specifications, and employ STL semantics to design the reward functions for RL. In these methods, the control policy synthesis problem for an STL specification can be formalized as follows.

Problem 1 (Control policy synthesis problem of STL semantics): Let φ be an STL specification that describes a task. Given an MDP model of the system $\mathcal{M} = \langle S, A, P, R_{\rho} \rangle$, where P is unknown and the reward R_{ρ} is designated by a specific robust semantics $\tilde{\rho}$. The objective is to synthesize a control policy π^* , such that the expected robustness values of all state trajectories ω in $\mathcal{D}_{\mathcal{M}}^{\pi^*}$ w.r.t. φ gets maximized. Mathematically,

$$\pi^* = \arg \max_{\pi} \mathbb{E}_{\omega \sim \mathcal{D}_{\mathcal{M}}^{\pi}} [\tilde{\rho}(\omega, \varphi, 0)]. \quad (2)$$

Note that R_{ρ} can be defined over multiple STL semantics, yielding different reward functions.

As we described in the introduction, robust semantics and its derived approximation semantics have already been explored to solve the above control problem [15], [17], [18]. However,

the robust semantics leads to the information masking problem [19]–[21], [25], which means that it may fail to report new violations or accurately describe the system’s evolution at the current instant after the first violation. When robust semantics is applied in RL, the masked information leads to sparse, inaccurate, and non-ideal rewards, which will degrade the performance of RL and hinder policy convergence. Therefore, existing RL methods based on STL robust semantics may suffer from the information masking problem.

III. ONLINE CAUSATION-GUIDED RL METHOD

In order to solve the problems of existing STL-guided RL methods, we propose the causation-guided RL method, which mainly consists of 1) generating RL rewards with the online causation semantics of STL in order to solve the problem of information masking of the existing STL’s robust semantics, and 2) defining the environment model as τ -MDP in order to solve the problem of non-Markovianity.

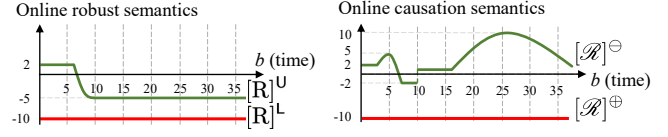
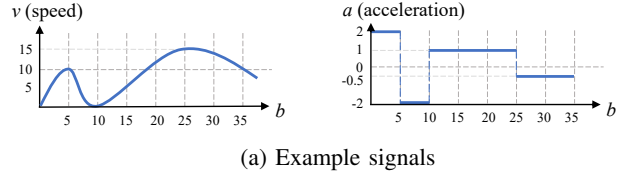
A. Online Causation Semantics of STL

To solve the information masking problem, [21] proposed the STL causation semantics, which is able to provide more information on the system evolution than the STL robust semantics. Given a partial signal $\mathbf{v}_{0:b}$ from time 0 to the current instant b , the causation semantics calculates a *violation causation distance* $[\mathcal{R}]^\ominus$ and a *satisfaction causation distance* $[\mathcal{R}]^\oplus$, which, respectively, indicate how far the signal value (the trajectory state) at the current instant b is from turning b into a violation/satisfaction causation instant such that b is relevant to the violation/satisfaction of a given STL formula.

In this paper, since we only use the violation causation distance (explained in Section IV-A), we present the causation semantics as follows by omitting the satisfaction causation distance. The full definition can be found in [21].

Definition 5 (Online causation semantics of STL): Let $\mathbf{v}_{0:b}$ be a partial signal from the initial instant 0 to the current instant b , and φ be an STL formula. At instant b , the violation causation distance $[\mathcal{R}]^\ominus(\mathbf{v}_{0:b}, \varphi, \mu)$ can be computed as follows:

$$\begin{aligned}
[\mathcal{R}]^\ominus(\mathbf{v}_{0:b}, \alpha, \mu) &:= \begin{cases} f(\mathbf{v}_{0:b}(\mu)) & \text{if } b = \mu \\ \mathbf{R}_{\max}^\alpha & \text{otherwise} \end{cases} \\
[\mathcal{R}]^\ominus(\mathbf{v}_{0:b}, \neg\varphi, \mu) &:= -[\mathcal{R}]^\oplus(\mathbf{v}_{0:b}, \varphi, \mu) \\
[\mathcal{R}]^\ominus(\mathbf{v}_{0:b}, \varphi_1 \wedge \varphi_2, \mu) &:= \\
&\min([\mathcal{R}]^\ominus(\mathbf{v}_{0:b}, \varphi_1, \mu), [\mathcal{R}]^\ominus(\mathbf{v}_{0:b}, \varphi_2, \mu)) \\
[\mathcal{R}]^\ominus(\mathbf{v}_{0:b}, \varphi_1 \vee \varphi_2, \mu) &:= \\
&\min\left(\max([\mathcal{R}]^\ominus(\mathbf{v}_{0:b}, \varphi_1, \mu), [\mathbf{R}]^\mathbf{U}(\mathbf{v}_{0:b}, \varphi_2, \mu)), \right. \\
&\left. \max([\mathbf{R}]^\mathbf{U}(\mathbf{v}_{0:b}, \varphi_1, \mu), [\mathcal{R}]^\ominus(\mathbf{v}_{0:b}, \varphi_2, \mu))\right) \\
[\mathcal{R}]^\ominus(\mathbf{v}_{0:b}, \square_I\varphi, \mu) &:= \inf_{t \in \mu+I} ([\mathcal{R}]^\ominus(\mathbf{v}_{0:b}, \varphi, t)) \\
[\mathcal{R}]^\ominus(\mathbf{v}_{0:b}, \diamond_I\varphi, \mu) &:= \\
&\inf_{t \in \mu+I} \left(\max([\mathcal{R}]^\ominus(\mathbf{v}_{0:b}, \varphi, t), [\mathbf{R}]^\mathbf{U}(\mathbf{v}_{0:b}, \diamond_I\varphi_2, \mu)) \right)
\end{aligned}$$



(b) The illustrations for the corresponding online causation semantics and robust semantics

Fig. 1: The comparison of online causation semantics and robust semantics against STL specification $\varphi = \square_{[0,100]}(v > 5 \vee a > 0)$.

$$\begin{aligned}
[\mathcal{R}]^\ominus(\mathbf{v}_{0:b}, \varphi_1 \mathbf{U}_I \varphi_2, \mu) &:= \\
\inf_{t \in \mu+I} \left(\max \left(\min \left(\inf_{t' \in [\mu, t]} [\mathcal{R}]^\ominus(\mathbf{v}_{0:b}, \varphi_1, t'), \right. \right. \right. \\
&\left. \left. \left. [\mathcal{R}]^\ominus(\mathbf{v}_{0:b}, \varphi_2, t) \right), [\mathbf{R}]^\mathbf{U}(\mathbf{v}_{0:b}, \varphi_1 \mathbf{U}_I \varphi_2, \mu) \right) \right).
\end{aligned}$$

Intuitively, violation causation distance $[\mathcal{R}]^\ominus(\mathbf{v}_{0:b}, \varphi, \mu)$ represents the spatial distance of the signal value $\mathbf{v}_{0:b}$, at the current instant b , from turning b into a violation causation instant such that b is relevant to the violation of φ (also applied to the satisfaction case dually). In this way, the causation semantics reflects the instantaneous status of system evolution more faithfully than robust semantics. Here is a simple example of computing the satisfaction causation distance.

Example 1: Figure 1a presents a vehicle’s speed and acceleration signals. The specification requires that the vehicle always accelerates or its speed is always greater than 5. For convenience, we name the sub-formulas of φ as follows:

$$\alpha_1 \equiv v > 5, \quad \alpha_2 \equiv a > 0, \quad f_1 \equiv v - 5, \quad f_2 \equiv a$$

At $b = 25$, the violation causation distance is computed as:

$$\begin{aligned}
[\mathcal{R}]^\ominus(\mathbf{v}_{0:5}, \varphi, 0) &= \inf_{t \in [0, 100]} [\mathcal{R}]^\ominus(\mathbf{v}_{0:5}, \alpha_1 \vee \alpha_2, t) \\
&= \inf_{t \in [0, 100]} \left(\min \left(\max([\mathcal{R}]^\ominus(\mathbf{v}_{0:5}, \alpha_1, t), [\mathbf{R}]^\mathbf{U}(\mathbf{v}_{0:5}, \alpha_2, t)), \right. \right. \\
&\left. \left. \max([\mathbf{R}]^\mathbf{U}(\mathbf{v}_{0:5}, \alpha_1, t), [\mathcal{R}]^\ominus(\mathbf{v}_{0:5}, \alpha_2, t)) \right) \right) \\
&= \min \left(\max([\mathcal{R}]^\ominus(\mathbf{v}_{0:5}, \alpha_1, 5), [\mathbf{R}]^\mathbf{U}(\mathbf{v}_{0:5}, \alpha_2, 5)), \right. \\
&\left. \max([\mathbf{R}]^\mathbf{U}(\mathbf{v}_{0:5}, \alpha_1, 5), [\mathcal{R}]^\ominus(\mathbf{v}_{0:5}, \alpha_2, 5)) \right) \\
&= \min \left(\max(f_1(10), f_2(-2)), \right. \\
&\left. \max(f_1(10), f_2(-2)) \right) \\
&= \max(f_1(10), f_2(-2)) = \max(5, -2) = 5
\end{aligned}$$

Figure 1b shows a comparison between the corresponding online robust semantics and the causation semantics.

Intuitively, in the interval $[20, 25]$, the system should satisfy the specification “more”, as the vehicle accelerates and the speed increases. We can see the causation semantics reflects the system evaluation as $[\mathcal{R}]^\ominus$ increases in $[20, 25]$. However,

robust semantic $[R]^U$ is monotonic and masks that as shown in the figure.

For the sake of simplicity, we use $\bar{\rho}$ to uniformly denote the violation causation distance or the satisfaction causation distance in the rest of this paper. Note that the causation concept is not in the scope of the well-known causality theory [26]. More details can be found in [21].

B. System Model

In regular RL problems, the system is usually modeled as an MDP. However, in STL-guided RL methods, rewards are given based on a state trajectory rather than a single state. Thus, as noted in [15], the RL algorithm cannot be applied to the original MDP, as the reward function is non-Markovian. To address this issue, we model the system as the τ -MDP proposed in [15], which aggregates the state trajectories of the original MDP into new states.

Definition 6 (τ -MDP): Given an MDP $\mathcal{M} = \langle S, A, P, R \rangle$ and a positive integer $k \geq 2$ as state aggregation value, a τ -MDP is a tuple $\mathcal{M}^\tau = \langle S^\tau, A, P^\tau, R^\tau \rangle$, where

- $S^\tau \subseteq (S)^k$ is a set of states, Each state $s^\tau \in S^\tau$ corresponds to a k -length trajectory on S . For an integer $t \in \mathbb{N}$, if $t \geq k - 1$, $s_t^\tau = s_{t-k+1:t}$, otherwise $s_t^\tau = (s_0)^{k-t-1} \cdot s_{0:t}$;
- A is a finite set of input actions, which is the same as that in \mathcal{M} ;
- $P^\tau : S^\tau \times A \times S^\tau \rightarrow [0, 1]$ is the probabilistic transition function. For any $s_t^\tau, s_{t+1}^\tau \in S^\tau$ and $a_t \in A$, $P^\tau(s_t^\tau, a, s_{t+1}^\tau) = P(s_t, a, s_{t+1})$ if $s_t^\tau(1, k - 1) = s_{t+1}^\tau(0, k - 2)$, $P^\tau(s_t^\tau, a, s_{t+1}^\tau) = 0$ otherwise,
- $R^\tau : S^\tau \rightarrow \mathbb{R}$ is a real-valued reward function.

Intuitively, τ -MDP treats the final k step trajectory as an entire state, where k is determined case by case. The trajectory of a τ -MDP is denoted as $\hat{\omega}$, each element $\hat{\omega}(i)$ is a k -length state trajectory. Accordingly, we denote the policy as $\hat{\pi} : S^\tau \rightarrow \text{Dist}(A)$ and the DTMC as $\mathcal{D}_{\mathcal{M}^\tau}^{\hat{\pi}} = \langle \bar{S}^\tau, \bar{P}^\tau \rangle$.

Furthermore, there exists a one-to-one correspondence between the trajectories in τ -MDP and the trajectories in the original MDP. Formally, let $\Sigma := \{\omega \mid (s_0, s_1, \dots, s_n), s_i \in S\}$, and $\Sigma_{\hat{\pi}}^\tau = \{\hat{\omega} \mid \hat{\omega} \sim \mathcal{D}_{\mathcal{M}^\tau}^{\hat{\pi}}\}$, then define

$$\mathcal{H} : \Sigma_{\hat{\pi}}^\tau \rightarrow \Sigma$$

$$\hat{\omega} \mapsto (\hat{\omega}(0)(-1), \hat{\omega}(1)(-1), \dots, \hat{\omega}(n)(-1))$$

Intuitively, this says for a trajectory ω in an original MDP, if $\text{len}(\omega) = \text{len}(\hat{\omega})$ and $\omega(i) = \hat{\omega}(i)(-1)$ for all $i \in \{0, \dots, \text{len}(\omega) - 1\}$, then ω is called the original trajectory of $\hat{\omega}$. According to Kolmogorov extension theorem, there exists a probability measure $\lambda_{\bar{P}^\tau}$ over $\Sigma_{\hat{\pi}}^\tau$, the map \mathcal{H} pushes probability $\lambda_{\bar{P}^\tau}$ into Σ , entails probability measure $\lambda_{\bar{P}^\tau} \circ \mathcal{H}^{-1}$. We denote $\mathcal{D}_{\mathcal{M}}^{\hat{\pi}}$ the probability space $(\Sigma, \lambda_{\bar{P}^\tau} \circ \mathcal{H}^{-1})$.

Note that, the τ -trajectory $\hat{\omega}$ does not conform to the format of input to STL semantics, and $\hat{\omega}$ needs to be reduced to the original trajectory for semantic interpretation. That is, for a certain STL semantics $\tilde{\rho}$, there is $\tilde{\rho}(\hat{\omega}, \varphi) = \tilde{\rho}(\omega, \varphi)$, where ω

is the original trajectory of $\hat{\omega}$, and we extend the definition of $\tilde{\rho}$ over τ -trajectory. We have the following conclusion.

Theorem 1 (Optimality transfer): Let $\hat{\pi}^*$ be any optimal policy in τ -MDP. Then, executing $\hat{\pi}^*$ in the original MDP also maximizes the expected STL semantic value $\tilde{\rho}(\omega, \varphi)$ of the original MDP, where ω is an arbitrary trajectory generated by executing a τ -MDP's policy in the original MDP, and φ is the given STL specification.

Proof. For a given original MDP \mathcal{M} and its extended τ -MDP, as well as a certain STL semantics $\tilde{\rho}$, the optimal policy $\hat{\pi}^*$ of the τ -MDP is:

$$\hat{\pi}^* = \arg \max_{\hat{\pi}} \mathbb{E}_{\hat{\omega} \sim \mathcal{D}_{\mathcal{M}^\tau}^{\hat{\pi}}} [\tilde{\rho}(\hat{\omega}, \varphi)], \quad (3)$$

Since $\tilde{\rho}(\hat{\omega}, \varphi) = \tilde{\rho}(\omega, \varphi)$ where ω is the original trajectory of $\hat{\omega}$, i.e., $\text{len}(\omega) = \text{len}(\hat{\omega})$ and $\omega(i) = \hat{\omega}(i)(-1)$ for all $i \in \{0, \dots, \text{len}(\omega) - 1\}$, we can get from Equation (3):

$$\hat{\pi}^* = \arg \max_{\hat{\pi}} \mathbb{E}_{\hat{\omega} \sim \mathcal{D}_{\mathcal{M}^\tau}^{\hat{\pi}}} [\tilde{\rho}(\omega, \varphi)]. \quad (4)$$

Let $\Sigma_{\hat{\pi}^*}^\tau = \{\hat{\omega} \mid \hat{\omega} \sim \mathcal{D}_{\mathcal{M}^\tau}^{\hat{\pi}^*}\}$ be the set of all trajectories generated by $\hat{\pi}^*$ executed on \mathcal{M}^τ , and let $\mathcal{D}_{\mathcal{M}}^{\hat{\pi}^*}$ be the induced probability space. Then $\Sigma_{\hat{\pi}^*} = \{\omega \mid \omega \sim \mathcal{D}_{\mathcal{M}}^{\hat{\pi}^*}\}$ denote the set of all trajectories generated by $\hat{\pi}^*$ executed on the original MDP \mathcal{M} . According to the definition of \mathcal{H} , for any $\hat{\omega} \in \Sigma_{\hat{\pi}^*}^\tau$, there exists one and only one $\omega \in \Sigma_{\hat{\pi}^*}$ corresponding to it. So we can get from Equation (4):

$$\hat{\pi}^* = \arg \max_{\hat{\pi}} \mathbb{E}_{\omega \sim \mathcal{D}_{\mathcal{M}}^{\hat{\pi}^*}} [\tilde{\rho}(\omega, \varphi)]. \quad (5)$$

Therefore, Theorem 1 holds. \square

C. Causation-Guided RL Method

In our online causation-guided RL method, for a given MDP model of the system $\mathcal{M} = \langle S, A, P, R \rangle$, the objective of the Problem 1 is to generate a good enough control policy π^* , so that the expected causation distance values of all state trajectories ω in $\mathcal{D}_{\mathcal{M}}^{\pi^*}$ with respect to specification φ get maximized. Based on Theorem 1 and [15, Theorem 4.2], the control synthesis problem in the MDP model can be transformed into the problem in the τ -MDP model, i.e., the expected semantic value yielded by π^* is bounded by that yielded by $\hat{\pi}^*$. We formalize our problem as follows.

Problem 2 (Control policy synthesis problem of STL causation semantics): Let φ be an STL specification for the system. Given a τ -MDP model of the system $\mathcal{M}^\tau = \langle S^\tau, A, P^\tau, R^\tau \rangle$, where P^τ is unknown and R^τ is given by the online causation semantics of STL. The objective is synthesizing a controller to generate a good enough control policy $\hat{\pi}^*$, so that the expected violation causation distances of all trajectories $\hat{\omega}$ in $\mathcal{D}_{\mathcal{M}^\tau}^{\hat{\pi}^*}$ w.r.t φ gets maximized. Mathematically,

$$\hat{\pi}^* = \arg \max_{\hat{\pi}} \mathbb{E}_{\hat{\omega} \sim \mathcal{D}_{\mathcal{M}^\tau}^{\hat{\pi}}} [\tilde{\rho}(\hat{\omega}, \varphi)]. \quad (6)$$

Now, we need to optimize Equation (6) with the RL algorithm to obtain the optimal policy. The implementation details and algorithm are discussed in Section IV.

IV. LEARNING APPROACH AND ALGORITHM

In this section, we give a concrete implementation of solving Problem 2 with the RL algorithm, including some technical details and the setting of the reward function.

A. Target Specification

A specification of a control system is typically characterized by a combination of safety (bad things never happen) and liveness (good things eventually happen) properties [27], [28]. The safety specification is typically represented by an expression shaped like $\Box_{[0,T]}\varphi_1$, while the liveness property can be represented as $\Diamond_{[0,T]}\varphi_2$, where T is a real number denoting a sufficiently large time step and also the maximum running time step of an episode of RL. However, since real systems do not run infinitely and some scenarios require more stringent time constraints on liveness, i.e., bounded liveness [29], the liveness property is denoted as $\Diamond_{[0,t]}\varphi_2$ in the STL specification, where $t \ll T$. After time t , the liveness specifications will no longer impact the quantitative semantics of the entire STL specification, which will lead to a very low influence of the liveness specifications in RL (only meaningful for time $[0, t]$).

To make the liveness specification more efficiently utilized in RL, we can nest a layer of \Box_I operators outside the liveness specification, then the liveness property becomes $\Box_I(\Diamond_{[0,t]}\varphi_2)$. Now, the liveness specification can be merged with the safety specification into $\Box_I(\Diamond_{[0,t]}\varphi_2 \wedge \varphi_1)$, which compare the form $\Box_I\varphi$, where $I = [0, T]$. Thus, it is sufficient to consider only the violation causation distance $[\mathcal{R}]^\ominus$, i.e., $\bar{\rho}(\hat{\omega}, \varphi) = [\mathcal{R}]^\ominus(\hat{\omega}, \varphi, 0)$ in Equation (6).

B. Sampling Window

Generally, the causation distance is computed based on the signal from time 0. However, as the running time of the system increases, the state trajectories lengthen, reducing the efficiency of causation distance calculation. To address this, we compute the causation distance for partial signals only. Inspired by the concept of the *horizon* [30] in STL, we define the *minimum sampling window* of the partial signal for an STL specification.

Definition 7 (STL minimum sampling window): Let $\mathbf{v}_{0:b}$ be a partial signal, and φ be an STL specification. The minimum sampling window $h(\mathbf{v}_{0:b}, \varphi)$ is defined as:

$$\begin{aligned} h(\mathbf{v}_{0:b}, \top) &= \emptyset, h(\mathbf{v}_{0:b}, \alpha) = \emptyset, \\ h(\mathbf{v}_{0:b}, \neg\varphi) &= h(\mathbf{v}_{0:b}, \varphi), \\ h(\mathbf{v}_{0:b}, \varphi_1 \wedge \varphi_2) &= h(\mathbf{v}_{0:b}, \varphi_1) \cup h(\mathbf{v}_{0:b}, \varphi_2), \\ h(\mathbf{v}_{0:b}, \varphi_1 \vee \varphi_2) &= h(\mathbf{v}_{0:b}, \varphi_1) \cup h(\mathbf{v}_{0:b}, \varphi_2), \\ h(\mathbf{v}_{0:b}, \Box_I\varphi) &= \begin{cases} I \cup h(\mathbf{v}_{0:b}, \varphi), & \text{if } b > \max(I) \\ \emptyset, & \text{otherwise} \end{cases}, \\ h(\mathbf{v}_{0:b}, \Diamond_I\varphi) &= \begin{cases} I \cup h(\mathbf{v}_{0:b}, \varphi), & \text{if } b > \max(I) \\ \emptyset, & \text{otherwise} \end{cases}, \\ h(\mathbf{v}_{0:b}, \varphi_1 \mathcal{U}_I \varphi_2) &= \begin{cases} I \cup h(\mathbf{v}_{0:b}, \varphi_1) \cup h(\mathbf{v}_{0:b}, \varphi_2), & \text{if } b > \max(I) \\ \emptyset, & \text{otherwise} \end{cases}. \end{aligned}$$

Note that it is sufficient that the sampling window H of the actual application can contain the minimum sampling window, i.e., $h(\mathbf{v}_{0:b}, \varphi) \subseteq H$ where $H = [0, u]$ is a positive closed interval. The violation causation distance of the signal within the sampling window H is denoted as $\bar{\rho}(\mathbf{v}_{b-H}, \varphi)$, where $b-H$ denotes the interval $[b-u, b]$ and \mathbf{v}_{b-H} represents the signal $\mathbf{v}_{b-u:b}$. In this case, the minimum state aggregation value of the system model is

$$k = \left\lceil \frac{u}{\Delta t} \right\rceil + 1, \quad (7)$$

where Δt is the time step and $\lceil \cdot \rceil$ is the ceiling function.

C. Methodology and Reward Function

To solve Problem 2 with the RL algorithm, i.e., find the optimal policy $\hat{\pi}^*$, we employ the parameterized policy $\hat{\pi}_\theta(a|s^\tau)$, which denotes the probability of selecting action a given state s^τ with parameter θ , i.e.

$$\hat{\pi}_\theta(a|s^\tau) = \mathbb{P}[a|s^\tau; \theta]. \quad (8)$$

The target function is associated with the policy parameter θ as follows:

$$J(\theta) = \mathbb{E}_{\hat{\omega} \sim \hat{\pi}_\theta} [\bar{\rho}(\hat{\omega}, \varphi)], \quad (9)$$

where $\mathbb{E}_{\hat{\omega} \sim \hat{\pi}_\theta}$ denotes the expectation operation over all traces $\hat{\omega}$ generated by using the policy $\hat{\pi}_\theta$.

Our goal is to learn a policy that maximizes the target function. Mathematically,

$$\theta^* = \arg \max_{\theta} J(\theta). \quad (10)$$

Hence, our optimal policy would be the one corresponding to θ^* , i.e., $\hat{\pi}_{\theta^*}$. We use an Actor-critic algorithm [31] to find the optimal policy. The gradient for the Actor (policy) can be approximated as follows:

$$\nabla_{\theta} J(\theta) = \mathbb{E}_{\hat{\pi}_\theta} \left[\sum_{t=0}^{T-1} \nabla_{\theta} \log \hat{\pi}_\theta(a_t | s_t^\tau) \cdot Q_\theta(s_t^\tau, a_t) \right], \quad (11)$$

where the Q-function of the actor $Q_\theta(s_t^\tau, a_t)$ is given as:

$$Q_\theta(s_t^\tau, a_t) = \mathbb{E}_{\hat{\pi}_\theta} \left[\sum_{t'=t}^T \bar{\rho}(s_{t'}^\tau, \varphi) | s_t^\tau, a_t \right]. \quad (12)$$

Therefore, the reward function is defined as

$$R^\tau(s^\tau) = \bar{\rho}(s^\tau, \varphi). \quad (13)$$

The policy gradient, given by Equation (11), is used to find the optimal policy. The critic, on the other hand, uses another action-value function $Q^\eta(s_t^\tau, a_t)$ to estimate the Q-function $Q_\theta(s_t^\tau, a_t)$ of the actor.

D. Smooth Approximation of Online Causation Semantics

The Q-value significantly influences the types of policies that can be expressed and regions that can be explored in RL. In fact, smoother Q-values play a crucial role in RL [32] as they lead to smoother policies [33]. However, the current Q-value in Equation (12) lacks smoothness due to the non-smooth reward function $\bar{\rho}(s_t^\tau, \varphi)$. For instance, consider the example in Figure 1, the violation causation distance curves exhibit the characteristics of a piecewise function, which is non-smooth at segmentation points. This lack of smoothness primarily arises from the max and min functions within the semantics, where an increase (or decrease) of a single value does not affect the result of the max and min functions, unless it is the minimum (or maximum) value.

Therefore, we use the log-sum-exp [34] approximation to smooth the max and min functions in the causation semantics, i.e.,

$$\max(x_1, \dots, x_n) \sim \frac{1}{\beta} \log \sum_{i=1}^n e^{\beta x_i}, \quad (14)$$

$$\min(x_1, \dots, x_n) \sim -\frac{1}{\beta} \log \sum_{i=1}^n e^{-\beta x_i}, \quad (15)$$

where $\beta > 0$ is a user-defined parameter and

$$\begin{aligned} \max(x_1, \dots, x_n) &\leq \frac{1}{\beta} \log \sum_{i=1}^n e^{\beta x_i} \\ &\leq \max(x_1, \dots, x_n) + \frac{1}{\beta} \log n, \end{aligned} \quad (16)$$

$$\begin{aligned} \min(x_1, \dots, x_n) &\geq -\frac{1}{\beta} \log \sum_{i=1}^n e^{-\beta x_i} \\ &\geq \min(x_1, \dots, x_n) - \frac{1}{\beta} \log n. \end{aligned} \quad (17)$$

Note that $\frac{1}{\beta} \log \sum_{i=1}^n e^{\beta x_i}$ and $-\frac{1}{\beta} \log \sum_{i=1}^n e^{-\beta x_i}$ can approximate the max and min function with arbitrary accuracy by selecting a large β . However, a larger β value will not always be better, as a large β may cause the approximation function to lose differentiability.

E. Online Causation-Guided RL Algorithm

The solution to Problem 2 can be summarized as Algorithm 1. A run of a system from start to end is called an *episode*. The inputs to the algorithm are the randomly initialized actor parameter θ and critic parameter η , the learning rates α_θ for actor and α_η for critic, the discount factor γ , and the sampling length k (calculated by Equation (7)).

We explain the steps of the algorithm as follows:

- 1) For each episode, initialize the state s_0^τ of τ -MDP (introduced in Section III-B) and assign it to the current state s_t^τ (Line 2-3).
- 2) For each step in an episode, first select the current action a_t according to the current policy $\hat{\pi}_\theta$, after which execute the action a_t and observe the next state s_{t+1}^τ (Line 5-6).

Algorithm 1 Online Causation-Guided RL Algorithm

Input: Actor parameters θ , critic parameters η ; learning rates α_θ (actor) and α_η (critic); discount factor $0 \leq \gamma < 1$; sampling length k .

- 1: **for** each episode **do**
 - 2: Initialize state $s_0, s_0^\tau = (s_0)^k$;
 - 3: Current state $s_t^\tau = s_0^\tau$;
 - 4: **for** $t = 0, 1, 2, \dots$ until termination **do**
 - 5: Sample action $a_t \sim \hat{\pi}_\theta(\cdot | s_t^\tau)$;
 - 6: Execute a_t and observe next state s_{t+1}^τ ;
 - 7: Compute reward $r^\tau = R^\tau(s_{t+1}^\tau)$;
 # R^τ is the smooth causation semantics
 - 8: Sample the next action: $a' = \hat{\pi}_\theta(\cdot | s_{t+1}^\tau)$;
 - 9: Compute temporal-difference error for action-value at time t :
 $\delta_t \leftarrow r_t^\tau + \gamma Q_\eta(s_{t+1}^\tau, a') - Q_\eta(s_t^\tau, a_t)$;
 - 10: Update the parameters of the critic:
 $\eta \leftarrow \eta + \alpha_\eta \delta_t \nabla_\eta Q_\eta(s_t^\tau, a_t)$;
 - 11: Update the parameters of the actor:
 $\theta \leftarrow \theta + \alpha_\theta \nabla_\theta Q_\eta(s_t^\tau, \hat{\pi}_\theta(a_t | s_t^\tau))$;
 - 12: Update state $s_t^\tau \leftarrow s_{t+1}^\tau$
-

- 3) Then the reward for the next state is computed. Note that the reward function here is a smooth approximation of the STL online causation semantics (detailed in Section IV-D), taking the causation distance of the next τ -state (a k -step state sequence) as the reward (Line 7).
- 4) Finally, select the next action a_{t+1} according to the current policy $\hat{\pi}_\theta$, compute the temporal difference error, and update the network parameters of the critic and the actor (Line 8-11).

The algorithm will end after multiple episodes, and the resulting $\hat{\pi}_\theta$ is the synthesized control policy. Compared to regular actor-critic algorithms, the main differences in online causality-guided RL algorithms are that 1) the inputs to the actor and critic networks are the states of the τ -MDP, i.e., a sequence of states rather than a single state, and 2) the reward function is given by a smooth approximation of the STL causation semantics.

V. EXPERIMENTS

We have implemented a prototype tool for our method and conducted experiments to evaluate its effectiveness and compare it with other STL-guided RL methods. All experiments are performed on an Ubuntu 22.04 machine equipped with an Intel Core i7-2700F CPU, an NVIDIA GeForce RTX 3080 GPU, and 32GB of RAM. The evaluated artifact and the experimental data are available at <https://doi.org/10.5281/zenodo.16879140>.

A. Benchmarks

We utilize the OpenAI Gym platform [23] as simulators for CPSs. The experiments were conducted on four benchmarks

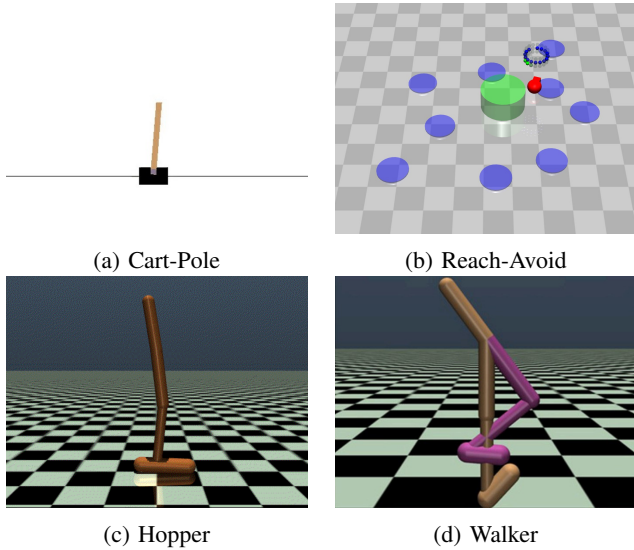


Fig. 2: Benchmarks used in experiments.

shown in Figure 2: Cart-Pole, Reach-Avoid, Hopper, and Walker. Each benchmark, along with its corresponding target STL specification, is described below.

a) Cart-Pole: The first benchmark is the classical Cart-Pole balancing problem described in [35], where a cart is controlled using a simple bang-bang controller that pushes it left or right. The state space of the environment is $(x, \dot{x}, \theta, \dot{\theta})$, where x is the displacement of the cart from the origin, \dot{x} is the speed of the cart, θ is the angle of displacement of the pole from the upright position, and $\dot{\theta}$ is the angular velocity of the pole rotation. The original target is to balance a pole on the cart for as long as possible. Our experiments have a more stringent target that can be formulated as the following STL specification:

$$\varphi = \square_{[0,\infty]}(\diamond_{[0,10]}(|\dot{x}| < 0.1) \wedge (|x| < 0.5) \wedge (|\theta| < 0.1)),$$

which means the cart has to achieve a position at $(-0.5, 0.5)$, a velocity less than 0.1, and an angle less than 0.1 in 10 steps for any moment.

b) Reach-Avoid: The Reach-Avoid benchmark presents a typical reach-avoid problem on the Safety Gym platform [36], where a point navigates to a green goal while avoiding contact with the 9 unsafe hazards on the map. The point has 44 states, including 16 states that represent Lidars that detect the distance and direction to the goal, and another 16 states measure the distance to hazards. The target of the experiment is that the point has to keep a safe distance from the hazards all the time and reach the goal range in 40 steps. The target can be formulated into the following STL specification:

$$\varphi = \square_{[0,\infty]}(\diamond_{[0,40]}(d_g \leq r_g) \wedge (d_c > r_c))$$

where d_g is the distance to the goal, d_c is the distance to the closest hazard, and $r_g = 0.3$ and $r_c = 0.2$ are the specified hazard radius and goal radius respectively. Both d_c and d_g are calculated from Lidar readings in the states.

c) Hopper: The third benchmark is derived from Mujoco environments [37]. The Hopper is a two-dimensional one-legged figure. The goal is to make hops that move in the forward (right) direction by applying torques on the three hinges connecting the four body parts. The state space of Hopper is an 11-dimensional array, including positional values, velocities, angles and angle velocities of different body parts. If the height of the top part is greater than 0.7 and the angle is within the range $[-1, 1]$, then Hopper’s posture is considered healthy. The target of the experiment is that Hopper has to maintain a healthy posture all the time and reach a speed of 0.5 in 15 steps. The target can be formulated into the following STL specification:

$$\varphi = \square_{[0,\infty]}(\diamond_{[0,15]}(v_x > 0.5) \wedge (z > 0.7) \wedge (|a| < 1))$$

where v_x is the velocity of the top in the x-direction, z is the z-coordinate of the top and a is the angle of the top.

d) Walker: The last benchmark is also derived from Mujoco environments. The Walker is a two-dimensional two-legged figure. The goal is to coordinate both sets of feet, legs, and thighs to move in the forward (right) direction by applying torques on the six hinges connecting the six body parts. The Walker has 17 states, including positional values, velocities, angles and angle velocities of different body parts. If the height of the top part is within the range $[0.8, 2]$ and the angle is within the range $[-1, 1]$, then Walker’s posture is considered healthy. The target of the experiment is that the Walker has to maintain a healthy posture all the time and reach a speed of 0.5 in 15 steps. The target can be formulated into the following STL specification:

$$\varphi = \square_{[0,\infty]}(\diamond_{[0,15]}(v_x > 0.5) \wedge (0.8 < z < 2) \wedge (|a| < 1))$$

where v_x is the velocity of the top in the x-direction, z is the z-coordinate of the top and a is the angle of the top.

B. Experimental Setup

a) Training setting: We have implemented our causation-guided RL method using Stable-Baseline3 [38], a framework developed and maintained by OpenAI. Like other STL semantics, causation semantics can be combined with various RL algorithms. We follow the choices commonly adopted in the benchmarks [18], [36], [39], using the Proximal Policy Optimization (PPO) algorithm [40] to train the control policy for the Cart-Pole and Reach-Avoid benchmarks, while the state-of-the-art Actor-Critic (SAC) algorithm [41] is applied to the Hopper and Walker benchmarks. We integrate the smooth causation-STL semantics on top of the online monitoring tool Breach [42]. The parameter β of the log-sum-exp function for the STL causation semantics is set to 10 and the length of partial signals for each benchmark is calculated by Equation (7). Table I presents the maximum steps per episode, training episodes, and the structure of neural networks.

b) Evaluation settings: In this paper, we compare our causation-guided RL method (CAU) with the baseline RL method using the hand-crafted reward function (BAS) [38] and three most-related STL-guided RL methods, i.e., using

TABLE I: Settings of training parameters (m_{epi} : max step per episode, n_{total} : the number of total steps, lr : the learning rate, and $stru_{NN}$: the structure of the hidden layers of the neural network, i.e., the number of nodes per layer).

Benchmark	m_{epi}	n_{epi}	lr	$stru_{NN}$
Cart-Pole	500	500	4e-4	[64, 64]
Reach-Avoid	1000	500	1e-5	[1024, 512, 512]
Hopper	1000	1600	3e-4	[64, 64]
Walker	1000	1600	3e-4	[64, 64]

classic robust semantics directly (**CLS**) [22], [42], log-sum-exp approximation of STL robust semantics (**LSE**) [43] and Smoothed-Summation-Subtraction approximation of STL robust semantics (**SSS**) [18]. These types of semantics have also been implemented on top of Breach [42].

Let T denote the length of a single episode, and φ denote the given STL specification. We use several metrics to measure the performance of each method:

- *Success or Failure (S/F)* [36]. If the training results converge and achieve the training goal (note that strict satisfaction of the given specification is not required), it is considered a success S; otherwise, it is considered a failure F.
- *Full Satisfaction (Full-SAT)*. For the full specification φ , the Full-SAT for a whole episode of length T is defined as Full-SAT = $\mathbb{I}[\rho(s_{0:T}, \varphi, 0)]$, where \mathbb{I} is an indicator function that equals 1 when the full specification φ is satisfied, i.e., $\rho(s_{0:T}, \varphi, 0) \geq 0$.
- *Safety Satisfaction (Safety-SAT)*. Let φ_s denote the safety component of the specification φ . The Safety-SAT for a full episode of length T is defined as Safety-SAT = $\mathbb{I}[\rho(s_{0:T}, \varphi_s, 0)]$, where \mathbb{I} is an indicator function that equals 1 when the safety component φ_s is satisfied, i.e., $\rho(s_{0:T}, \varphi_s, 0) \geq 0$.
- *Cost Return (CR)* [36]. The average cost return for N episodes is defined as $CR = \frac{1}{N} \sum_{i=0}^N \sum_{t=0}^T c_t$, where c_t is fixed for each step of safety violation in the environment. This metric can be interpreted as the average policy’s performance in terms of safety violations. Therefore, the lower, the better.

Note that for the comparison of these methods, we first compare their S/F. For the successful methods, we then compare their Full-SAT, Safety-SAT and CR.

C. Experimental Results

For each benchmark, we perform training over 10 random seeds, and count the average rewards per 50 rounds for each training. Figure 3 and Figure 4 show the comparison of our method with baseline and our method with other STL-guided RL methods in the training process, respectively, where the folds are the mean values of the 10 trainings, and the shaded areas indicate the standard deviation. Due to the varying reward scales provided by different STL semantics, we

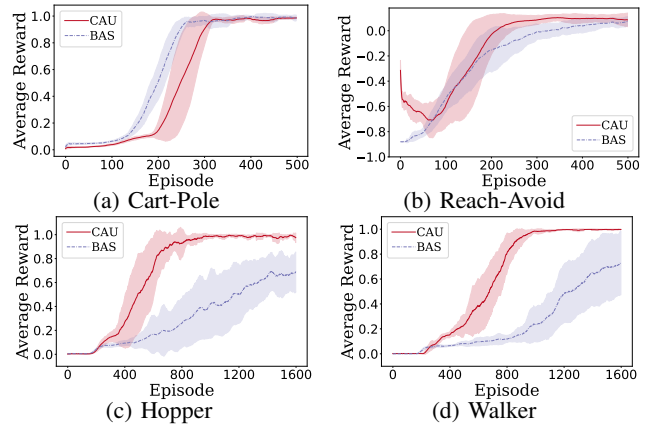


Fig. 3: Learning curves for training processes of CAU and BAS method.

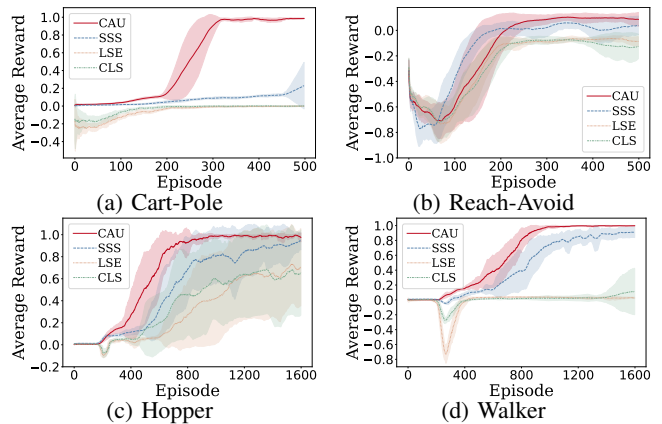


Fig. 4: Learning curves for training processes of CAU and other STL-guided method.

normalized the training results for each experiment. As illustrated by learning curves, our CAU method achieves favorable training outcomes across different benchmarks. Additionally, we have tested the synthesized controller on 100 distinct seeds to evaluate the training effectiveness of the methods. The test results are shown in Table II. It is intuitively obvious from the learning curves and evaluation table that CAU, SSS and BSA are clearly superior to the other two methods. In order to compare the three methods more objectively, we conducted statistical tests, and the results are shown in Table III. We adopt the Mann-Whitney U test [44] with $\alpha = 0.05$ as the confidence value of the null hypothesis of no significant difference; in case of a significant difference, we use Vargha and Delaney’s \hat{A}_{12} effect size [45] to assess the degree of significance.

From the training process and test results, we can observe that CAU outperforms other methods:

- In the Cart-Pole benchmark, only our CAU is able to converge (as shown in Figure 4a), while in this case, none of the other three STL-based methods could be trained successfully. Also, although BAS converges slightly faster than CAU, the evaluation is much worse for Full-SAT,

TABLE II: Experimental results of different methods under different environments.

Benchmark	Method	S/F	Full-SAT	Safety-SAT	CR
Cart-Pole	CAU	S	0.4290±0.3522	0.8520±0.1481	0.0031±0.0033
	SSS	F	-	-	-
	LSE	F	-	-	-
	CLS	F	-	-	-
	BAS	S	0.1020±0.2439	0.5430±0.3958	0.1536±0.2537
Reach-Avoid	CAU	S	0.0±0.0	0.4220±0.0890	0.0167±0.0153
	SSS	S	0.0±0.0	0.3680±0.1487	0.0298±0.0289
	LSE	S	0.0±0.0	0.3280±0.1025	0.0503±0.0390
	CLS	S	0.0±0.0	0.2320±0.1655	0.0533±0.0423
	BAS	S	0.0±0.0	0.4540±0.0486	0.0010±0.0019
Hopper	CAU	S	0.8270±0.2709	0.9520±0.1282	5.8e-6±1.57e-4
	SSS	S	0.6670±0.4246	0.8990±0.2997	0.0011±0.0034
	LSE	S	0.7780±0.3896	0.7780±0.3896	0.0014±0.0028
	CLS	S	0.6200±0.4376	0.6200±0.4376	0.0022±0.0030
	BAS	S	0.3540±0.3791	0.5540±0.4073	0.0050±0.0130
Walker	CAU	S	0.7120±0.2787	1.0±0.0	0.0±0.0
	SSS	S	0.3560±0.3821	0.9960±0.0066	4e-6±7e-6
	LSE	F	-	-	-
	CLS	F	-	-	-
	BAS	S	0.2090±0.2678	0.7570±0.3542	0.0005±0.0010

Safety-SAT and CR.

- In the Reach-Avoid benchmark, every STL-guided method converges and returns a controller. Although CAU converges more slowly than SSS, it has a more stable training effect, which is clearly shown in Figure 4b. In addition, CAU has also been evaluated to have higher safety assurance (higher Safety-SAT and lower CR) compared to other STL-based methods. The difference in evaluation values between CAU and BAS is also statistically negligible. The reason for Full-SAT being 0 in the evaluation results is that the initial state of the Point is too far from the target to reach it within 40 time-steps (it was tested to be reachable within about 200 time-steps).
- In the Hopper benchmark, all STL-guided methods successfully trained controllers. However, CAU converges fastest and most stably as shown in Figure 4c, and the obtained controller achieves higher Full-SAT and Safety-SAT, and lower CR.
- In the Walker benchmark, both CAU and SSS can successfully converge, while BAS has not yet completely converged. However, CAU converges faster and more stable than SSS as shown in Figure 4d, and achieves perfect Full-SAT, much higher Safety-SAT, and zero CR.

Overall, compared to the other three STL-based methods, our method has a 24%-100% improvement in Full-SAT, a 0.4%-14.7% improvement in Safety-SAT, and a 44%-100% decrease in CR.

D. Discussion

a) *Scalability*: Compared with other STL-guided RL methods, concerns about the additional overhead of CAU mainly involve two aspects: 1) whether computing the causation semantics introduces additional computational cost; and

TABLE III: Statistical testing of comparing CAU with BAS and SSS.

		BAS	SSS
Cart-Pole	Full-SAT	✓✓✓	✓✓✓
	Safety-SAT	✓✓	✓✓✓
	CR	✓✓	✓✓✓
Reach-Avoid	Full-SAT	-	-
	Safety-SAT	-	✓
	CR	-	✓✓✓
Hopper	Full-SAT	✓✓✓	✓
	Safety-SAT	✓✓✓	-
	CR	✓✓✓	-
Walker	Full-SAT	✓✓✓	✓✓
	Safety-SAT	✓✓✓	✓✓
	CR	✓✓✓	✓✓

negligible: - small better.: ✓ medium better.: ✓✓ large better.: ✓✓✓

TABLE IV: The average training time for per-step of different methods. Time is reported in seconds.

Benchmark	CAU	SSS	LSE	CLS
Cart-Pole	0.001996	0.001394	0.001174	0.001061
Reach-Avoid	0.006040	0.004140	0.003616	0.004056
Hopper	0.007829	0.005666	0.005353	0.005743
Walker	0.007656	0.005487	0.005856	0.005864

2) whether the use of τ -MDP leads to increased overhead. We analyze the scalability of the CAU method from these two aspects.

- 1) We adopt the latest implementation of CAU [46], which has shown that computing causation semantics takes the same magnitude of time as computing robust semantics,

TABLE V: Experimental results and average training time for per-step of different k .

Benchmark	k	Full-SAT	Safety-SAT	CR	per-step time (s)
Cart-Pole	11	0.4290±0.3522	0.8520±0.1481	3.104e-3±3.306e-3	0.001996
	16	0.2700±0.1647	0.6880±0.3212	1.281e-2±2.347e-2	0.002387
	21	0.1570±0.2514	0.4150±0.2777	1.678e-2±1.412e-2	0.003056
	26	0.1970±0.1818	0.6790±0.2238	7.399e-3±8.810e-3	0.003854
	31	0.1540±0.1973	0.5350±0.3065	2.328e-2±3.412e-2	0.004785
Hopper	16	0.8270±0.2709	0.9520±0.1282	5.770e-6±1.568e-4	0.007829
	21	0.9000±0.1522	1.0±0.0	0.0±0.0	0.008406
	26	0.8020±0.3176	1.0±0.0	0.0±0.0	0.009134
	31	0.8120±0.3420	0.9970±0.0064	3.012e-6±6.432e-6	0.001005
	36	0.8740±0.1581	0.9980±0.0040	2.001e-6±4.010e-6	0.001120

and therefore it does not introduce much overhead in comparison to classical robust semantics.

- 2) Although introducing the τ -MDP increases the computational cost of the neural networks (due to higher input dimension and larger replay buffer), the overhead is limited and only depends on the parameter k , which corresponds to the time bound of the liveness property—typically a small integer. Table IV summarizes the average per-step training time of CAU and other STL-guided RL methods. Although the use of τ -MDP increases the state dimensionality by a factor of 6 to 41 in different benchmarks, the per-step training time remains within the same order of magnitude.

b) Parameter: We further analyzed the impact of the parameter k on training performance and computational cost in the Cart-Pole and Hopper benchmarks. Based on the minimum sampling window, we conducted four additional experiments using larger sampling windows in increments of 5 time steps, and compiled the evaluation results and average single-step training time (as shown in Table V). The results indicate that

- 1) increasing k does not significantly improve training performance, and overly long historical state sequences may even introduce noise and hinder policy synthesis,
- 2) while training time increases sub-linearly with k (the power exponent is 0.85 for Cart-Pole and 0.43 for Hopper).

In general, the minimum sampling window can be used as the initial setting for k , while the optimal trade-off between computational cost and training performance may require case-by-case analysis.

VI. RELATED WORK

Model-free RL [14] has become a popular method for synthesizing controllers for unknown dynamic systems. In RL, the policy of an *agent* is trained based on feedback from a reward function, aiming to maximize cumulative reward. Therefore, a poorly designed reward function can lead to the development of policies that do not align with the intended objectives. In some RL-based controller synthesis approaches [47]–[51], the reward function is designed by a control engineer who has complete knowledge of the system dynamics. However, this

TABLE VI: Comparison with other RL reward generation methods

	Automation	Expressiveness	Quantification	Informativeness
Hand-crafted	✗	✓	✓	✓
LTL	✓✓✓	✓✓	✗	✓
TLTL	✓✓✓	✓✓✓	✓	✓
STL-robust	✓✓✓	✓✓✓	✓	✓✓
Ours	✓✓✓	✓✓✓	✓	✓✓✓

approach is often case-specific, and designing an appropriate reward function becomes increasingly challenging as the system’s dimensionality and nonlinearity increase. Moreover, in safety-critical systems, the agent may adopt policies that maximize the expected total rewards but produce unsafe or impractical operations; this phenomenon is known as *reward hacking* [52], [53].

Recent developments have applied temporal logic [3] to reward generation, guiding RL synthesis to obtain control policies that satisfy formal specifications. For instance, *linear temporal logic* (LTL)-guided model-free RL algorithms have been designed to maximize the probability of satisfying the formal specifications [54]–[57]. However, reward signals derived from LTL [58] specifications are typically sparse, which hinders the effectiveness of RL in complex tasks. Li et al. [43], [59] proposed *truncated linear temporal logic* (TLTL) with quantitative semantics and used its robustness degree as a reward function for RL, which improves the learning speed. Nevertheless, LTL still lacks the ability to describe real-time constraints.

In addition, plenty of works have explored the use of STL semantics to define reward functions for RL tasks. Aksaray et al. [15] applied STL robust semantics to reward generation in Q-learning. Kalagarla et al. [60] proposed an STL-guided RL method that considers performance constraints and two-layer nested temporal operators. However, these methods are based on offline semantics and lack extensions in deep-RL. Balakrishnan and Deshmukh proposed using STL robust semantics of partial signals to design a reward function for deep RL [17], but the robust semantics are still not smooth. Singh and Saha [18] proposed a smooth robust semantic over partial signals, showing good performance in guiding RL.

We list above reward assignment methods and our method with 5 attributes in TABLE VI, in which ✕ indicates non-conformity of the attributes and ✓ and its number indicates conformity of the attributes.

- Compared with baseline RL using *hand-crafted* rewards, the other 4 category methods are *formal specification*-based, which allows engineers to easily specify system requirements by formal languages; these formally-specified requirements can be **automatically** parsed and translated to rewards, saving significant efforts of hand-crafting rewards in a case-by-case manner.
- Compared with *LTL*-based rewards, besides STL's advantages in **expressiveness** [61], STL-based methods (last 2 columns) enable **quantification** of rewards, thereby exhibiting distinct strengths in **informativeness**.
- Other STL-guided RL methods still suffer from the information masking problem due to the monotonicity of STL robust semantics. Instead, our method leverages the online causation semantics of STL, which reflect the instantaneous status of system evolution more faithfully than robust semantics, and thus enjoy the benefits leading to more accurate rewards.

VII. CONCLUSION

We propose a novel causation-guided RL approach for controller synthesis of STL. The experimental results demonstrate that our approach outperforms the existing relevant STL-guided RL methods across multiple complex benchmarks. Although our method incurs a small amount of additional overhead, it is acceptable compared to the improvement in satisfaction of goal. For future work, we aim to investigate reward generation methods with lower computational overhead and higher goal satisfaction based on STL causation semantics, and to apply these techniques to practical cyber-physical systems such as autonomous vehicles.

ACKNOWLEDGMENTS

We thank the anonymous reviewers for their valuable comments, which significantly improved the quality of this paper. We also thank Shenghua Feng for his help in improving this paper. Xiaochen Tang and Miaomiao Zhang are supported by the Natural Science Foundation of China (NSFC) Grant No. 62472316 and No. 62032019. Zhenya Zhang is supported by the JSPS Grant No. JP25K21179 and JST BOOST Grant No. JPMJBY24D7. Jie An is supported by the National Key R&D Program of China under grants No. 2022YFA1005100, No. 2022YFA1005101 and No. 2022YFA1005103, the NSFC grants No. W2511064, No. 62192732 and No. 62032024, and the ISCAS Basic Research Grant No. ISCAS-JCZD202406.

REFERENCES

[1] R. Baheti and H. Gill, "Cyber-physical systems," *The impact of control technology*, vol. 12, no. 1, pp. 161–166, 2011.

[2] E. A. Lee, "Cyber physical systems: Design challenges," in *2008 11th IEEE International Symposium on Object and Component-Oriented Real-Time Distributed Computing (ISORC)*, 2008, pp. 363–369.

[3] A. Pnueli, "The temporal logic of programs," in *FOCS 1977, Providence, Rhode Island, USA, 31 October - 1 November 1977*. IEEE Computer Society, 1977, pp. 46–57. [Online]. Available: <https://doi.org/10.1109/SFCS.1977.32>

[4] A. Donzé and O. Maler, "Robust satisfaction of temporal logic over real-valued signals," in *FORMATS 2010, Klosterneuburg, Austria, September 8-10, 2010. Proceedings*, ser. Lecture Notes in Computer Science, vol. 6246. Springer, 2010, pp. 92–106. [Online]. Available: https://doi.org/10.1007/978-3-642-15297-9_9

[5] G. E. Fainekos and G. J. Pappas, "Robustness of temporal logic specifications for continuous-time signals," *Theor. Comput. Sci.*, vol. 410, no. 42, pp. 4262–4291, 2009. [Online]. Available: <https://doi.org/10.1016/j.tcs.2009.06.021>

[6] S. Jaksic, E. Bartocci, R. Grosu, T. Nguyen, and D. Nickovic, "Quantitative monitoring of STL with edit distance," *Formal Methods Syst. Des.*, vol. 53, no. 1, pp. 83–112, 2018. [Online]. Available: <https://doi.org/10.1007/s10703-018-0319-x>

[7] P. Jain, P. K. Aggarwal, P. Chaudhary, K. Makar, J. Mehta, and R. Garg, *Convergence of IoT and CPS in Robotics*. Cham: Springer International Publishing, 2021, pp. 15–30. [Online]. Available: https://doi.org/10.1007/978-3-030-66222-6_2

[8] M. Han, Z. Duan, and Y. Li, "Privacy issues for transportation cyber physical systems," *Secure and trustworthy transportation cyber-physical systems*, pp. 67–86, 2017.

[9] V. Raman, A. Donzé, M. Maasoumy, R. M. Murray, A. L. Sangiovanni-Vincentelli, and S. A. Seshia, "Model predictive control with signal temporal logic specifications," in *53rd IEEE Conference on Decision and Control, CDC 2014, Los Angeles, CA, USA, December 15-17, 2014*. IEEE, 2014, pp. 81–87. [Online]. Available: <https://doi.org/10.1109/CDC.2014.7039363>

[10] A. T. Buyukkocak, D. Aksaray, and Y. Yazicioglu, "Sequential control barrier functions for mobile robots with dynamic temporal logic specifications," *Robotics Auton. Syst.*, vol. 176, p. 104681, 2024. [Online]. Available: <https://doi.org/10.1016/j.robot.2024.104681>

[11] L. Lindemann and D. V. Dimarogonas, "Efficient automata-based planning and control under spatio-temporal logic specifications," in *2020 American Control Conference, ACC 2020, Denver, CO, USA, July 1-3, 2020*. IEEE, 2020, pp. 4707–4714. [Online]. Available: <https://doi.org/10.23919/ACC45564.2020.9147796>

[12] D. Gundana and H. Kress-Gazit, "Event-based signal temporal logic synthesis for single and multi-robot tasks," *IEEE Robotics Autom. Lett.*, vol. 6, no. 2, pp. 3687–3694, 2021. [Online]. Available: <https://doi.org/10.1109/LRA.2021.3064220>

[13] Q. H. Ho, R. B. Ilyes, Z. N. Sunberg, and M. Lahijanian, "Automaton-guided control synthesis for signal temporal logic specifications," in *61st IEEE Conference on Decision and Control, CDC 2022, Cancun, Mexico, December 6-9, 2022*. IEEE, 2022, pp. 3243–3249. [Online]. Available: <https://doi.org/10.1109/CDC51059.2022.9993090>

[14] R. S. Sutton and A. G. Barto, "Reinforcement learning: An introduction," *IEEE Trans. Neural Networks*, vol. 9, no. 5, pp. 1054–1054, 1998. [Online]. Available: <https://doi.org/10.1109/TNN.1998.712192>

[15] D. Aksaray, A. Jones, Z. Kong, M. Schwager, and C. Belta, "Q-learning for robust satisfaction of signal temporal logic specifications," in *55th IEEE Conference on Decision and Control, CDC 2016, Las Vegas, NV, USA, December 12-14, 2016*. IEEE, 2016, pp. 6565–6570. [Online]. Available: <https://doi.org/10.1109/CDC.2016.7799279>

[16] Q. Gao, D. Hajinezhad, Y. Zhang, Y. Kantaros, and M. M. Zavlanos, "Reduced variance deep reinforcement learning with temporal logic specifications," in *ICCP 2019, Montreal, QC, Canada, April 16-18, 2019*. ACM, 2019, pp. 237–248. [Online]. Available: <https://doi.org/10.1145/3302509.3311053>

[17] A. Balakrishnan and J. V. Deshmukh, "Structured reward shaping using signal temporal logic specifications," in *IROS 2019, Macau, SAR, China, November 3-8, 2019*. IEEE, 2019, pp. 3481–3486. [Online]. Available: <https://doi.org/10.1109/IROS40897.2019.8968254>

[18] N. K. Singh and I. Saha, "Stl-based synthesis of feedback controllers using reinforcement learning," in *AAAI 2023, Washington, DC, USA, February 7-14, 2023*. AAAI Press, 2023, pp. 15 118–15 126. [Online]. Available: <https://doi.org/10.1609/aaai.v37i12.26764>

[19] K. Selyunin, S. Jaksic, T. Nguyen, C. Reidl, U. Hafner, E. Bartocci, D. Nickovic, and R. Grosu, "Runtime monitoring with recovery of the SENT communication protocol," in *CAV 2017, Heidelberg, Germany, July 24-28, 2017, Proceedings, Part I*, ser. Lecture Notes in Computer

- Science, vol. 10426. Springer, 2017, pp. 336–355. [Online]. Available: https://doi.org/10.1007/978-3-319-63387-9_17
- [20] Z. Zhang, P. Arcaini, and X. Xie, “Online reset for signal temporal logic monitoring,” *IEEE Trans. Comput. Aided Des. Integr. Circuits Syst.*, vol. 41, no. 11, pp. 4421–4432, 2022. [Online]. Available: <https://doi.org/10.1109/TCAD.2022.3197693>
- [21] Z. Zhang, J. An, P. Arcaini, and I. Hasuo, “Online causation monitoring of signal temporal logic,” in *CAV 2023, Paris, France, July 17–22, 2023, Proceedings, Part I*, ser. Lecture Notes in Computer Science, vol. 13964. Springer, 2023, pp. 62–84. [Online]. Available: https://doi.org/10.1007/978-3-031-37706-8_4
- [22] J. V. Deshmukh, A. Donz , S. Ghosh, X. Jin, G. Juniwal, and S. A. Seshia, “Robust online monitoring of signal temporal logic,” *Formal Methods Syst. Des.*, vol. 51, no. 1, pp. 5–30, 2017. [Online]. Available: <https://doi.org/10.1007/s10703-017-0286-7>
- [23] G. Brockman, V. Cheung, L. Petterson, J. Schneider, J. Schulman, J. Tang, and W. Zaremba, “Openai gym,” *CoRR*, vol. abs/1606.01540, 2016. [Online]. Available: <http://arxiv.org/abs/1606.01540>
- [24] R. Bellman, “A markovian decision process,” *Journal of Mathematics and Mechanics*, vol. 6, no. 5, pp. 679–684, 1957. [Online]. Available: <http://www.jstor.org/stable/24900506>
- [25] A. Cimatti, C. Tian, and S. Tonetta, “Assumption-based runtime verification with partial observability and resets,” in *RV 2019, Porto, Portugal, October 8–11, 2019, Proceedings*. Berlin, Heidelberg: Springer-Verlag, 2019, p. 165–184. [Online]. Available: https://doi.org/10.1007/978-3-030-32079-9_10
- [26] J. Pearl, *Causality*. Cambridge university press, 2009.
- [27] B. Alpern and F. B. Schneider, “Recognizing safety and liveness,” *Distributed Comput.*, vol. 2, no. 3, pp. 117–126, 1987. [Online]. Available: <https://doi.org/10.1007/BF01782772>
- [28] E. Kindler, “Safety and liveness properties: A survey,” 2007. [Online]. Available: <https://api.semanticscholar.org/CorpusID:18452230>
- [29] L. Lamport, “Fairness and hyperfairness,” *Distributed Comput.*, vol. 13, no. 4, pp. 239–245, 2000. [Online]. Available: <https://doi.org/10.1007/PL00008921>
- [30] A. Dokhanchi, B. Hoxha, and G. Fainekos, “On-line monitoring for temporal logic robustness,” in *RV 2014, Toronto, ON, Canada, September 22–25, 2014, Proceedings*, ser. Lecture Notes in Computer Science, vol. 8734. Springer, 2014, pp. 231–246. [Online]. Available: https://doi.org/10.1007/978-3-319-11164-3_19
- [31] V. R. Konda and J. N. Tsitsiklis, “Onactor-critic algorithms,” *SIAM J. Control. Optim.*, vol. 42, pp. 1143–1166, 2003. [Online]. Available: <https://api.semanticscholar.org/CorpusID:207079270>
- [32] O. Nachum, M. Norouzi, G. Tucker, and D. Schuurmans, “Smoothed action value functions for learning gaussian policies,” in *ICML 2018, Stockholm, Sweden, July 10–15, 2018, ser. Proceedings of Machine Learning Research*, vol. 80. PMLR, 2018, pp. 3689–3697. [Online]. Available: <http://proceedings.mlr.press/v80/nachum18a.html>
- [33] Q. Shen, Y. Li, H. Jiang, Z. Wang, and T. Zhao, “Deep reinforcement learning with robust and smooth policy,” in *ICML 2020, 13–18 July 2020, Virtual Event*, ser. Proceedings of Machine Learning Research, vol. 119. PMLR, 2020, pp. 8707–8718. [Online]. Available: <http://proceedings.mlr.press/v119/shen20b.html>
- [34] M. Chen and M. Chiang, “Distributed optimization in networking: Recent advances in combinatorial and robust formulations,” in *Modeling and Optimization: Theory and Applications*. New York, NY: Springer New York, 2012, pp. 25–52.
- [35] A. G. Barto, R. S. Sutton, and C. W. Anderson, “Neuronlike adaptive elements that can solve difficult learning control problems,” *IEEE Trans. Syst. Man Cybern.*, vol. 13, no. 5, pp. 834–846, 1983. [Online]. Available: <https://doi.org/10.1109/TSMC.1983.6313077>
- [36] J. Achiam and D. Amodei, “Benchmarking safe exploration in deep reinforcement learning,” 2019. [Online]. Available: <https://api.semanticscholar.org/CorpusID:208283920>
- [37] E. Todorov, T. Erez, and Y. Tassa, “Mujoco: A physics engine for model-based control,” in *IROS 2012, Vilamoura, Algarve, Portugal, October 7–12, 2012*. IEEE, 2012, pp. 5026–5033. [Online]. Available: <https://doi.org/10.1109/IROS.2012.6386109>
- [38] A. Raffin, A. Hill, A. Gleave, A. Kanervisto, M. Ernestus, and N. Dormann, “Stable-baselines3: Reliable reinforcement learning implementations,” *J. Mach. Learn. Res.*, vol. 22, pp. 268:1–268:8, 2021. [Online]. Available: <http://jmlr.org/papers/v22/20-1364.html>
- [39] S. Jiang, M. Liu, and F. Kong, “Backdoor attacks on safe reinforcement learning-enabled cyber-physical systems,” *IEEE Trans. Comput. Aided Des. Integr. Circuits Syst.*, vol. 43, no. 11, pp. 4093–4104, 2024. [Online]. Available: <https://doi.org/10.1109/TCAD.2024.3447468>
- [40] J. Schulman, F. Wolski, P. Dhariwal, A. Radford, and O. Klimov, “Proximal policy optimization algorithms,” *CoRR*, vol. abs/1707.06347, 2017. [Online]. Available: <http://arxiv.org/abs/1707.06347>
- [41] T. Haarnoja, A. Zhou, P. Abbeel, and S. Levine, “Soft actor-critic: Off-policy maximum entropy deep reinforcement learning with a stochastic actor,” in *ICML 2018, Stockholm, Sweden, July 10–15, 2018, ser. Proceedings of Machine Learning Research*, vol. 80. PMLR, 2018, pp. 1856–1865. [Online]. Available: <http://proceedings.mlr.press/v80/haarnoja18b.html>
- [42] A. Donz , “Breach, A toolbox for verification and parameter synthesis of hybrid systems,” in *CAV 2010, Edinburgh, UK, July 15–19, 2010, Proceedings*, ser. Lecture Notes in Computer Science, vol. 6174. Springer, 2010, pp. 167–170. [Online]. Available: https://doi.org/10.1007/978-3-642-14295-6_17
- [43] X. Li, Y. Ma, and C. Belta, “A policy search method for temporal logic specified reinforcement learning tasks,” in *ACC 2018, Milwaukee, WI, USA, June 27–29, 2018*. IEEE, 2018, pp. 240–245. [Online]. Available: <https://doi.org/10.23919/ACC.2018.8431181>
- [44] H. B. Mann and D. R. Whitney, “On a test of whether one of two random variables is stochastically larger than the other,” *The annals of mathematical statistics*, pp. 50–60, 1947.
- [45] A. Vargha and H. D. Delaney, “A critique and improvement of the cl common language effect size statistics of mcgraw and wong,” *Journal of Educational and Behavioral Statistics*, vol. 25, no. 2, pp. 101–132, 2000.
- [46] Z. Zhang, J. An, P. Arcaini, and I. Hasuo, “Caumon: An informative online monitor for signal temporal logic,” in *Formal Methods - 26th International Symposium, FM 2024, Milan, Italy, September 9–13, 2024, Proceedings, Part II*, ser. Lecture Notes in Computer Science, A. Platzer, K. Y. Rozier, M. Pradella, and M. Rossi, Eds., vol. 14934. Springer, 2024, pp. 286–304. [Online]. Available: https://doi.org/10.1007/978-3-031-71177-0_18
- [47] T. P. Lillicrap, J. J. Hunt, A. Pritzel, N. Heess, T. Erez, Y. Tassa, D. Silver, and D. Wierstra, “Continuous control with deep reinforcement learning,” in *ICLR 2016, San Juan, Puerto Rico, May 2–4, 2016, Conference Track Proceedings*, 2016. [Online]. Available: <http://arxiv.org/abs/1509.02971>
- [48] S. Levine and V. Koltun, “Guided policy search,” in *ICML 2013, Atlanta, GA, USA, 16–21 June 2013, ser. JMLR Workshop and Conference Proceedings*, vol. 28. JMLR.org, 2013, pp. 1–9. [Online]. Available: <http://proceedings.mlr.press/v28/levine13.html>
- [49] M. P. Deisenroth, G. Neumann, and J. Peters, “A survey on policy search for robotics,” *Found. Trends Robotics*, vol. 2, no. 1–2, pp. 1–142, 2013. [Online]. Available: <https://doi.org/10.1561/23000000021>
- [50] N. Fulton and A. Platzer, “Safe reinforcement learning via formal methods: Toward safe control through proof and learning,” in *AAAI 2018, New Orleans, Louisiana, USA, February 2–7, 2018*. AAAI Press, 2018, pp. 6485–6492. [Online]. Available: <https://doi.org/10.1609/aaai.v32i1.12107>
- [51] R. Hafner and M. A. Riedmiller, “Reinforcement learning in feedback control - challenges and benchmarks from technical process control,” *Mach. Learn.*, vol. 84, no. 1–2, pp. 137–169, 2011. [Online]. Available: <https://doi.org/10.1007/s10994-011-5235-x>
- [52] D. Hadfield-Menell, S. Milli, P. Abbeel, S. J. Russell, and A. D. Dragan, “Inverse reward design,” in *NIPS 2017, December 4–9, 2017, Long Beach, CA, USA, 2017*, pp. 6765–6774. [Online]. Available: <https://proceedings.neurips.cc/paper/2017/hash/32fdab6559cdfa4f167f8c31b9199643-Abstract.html>
- [53] Y. Yuan, Z. L. Yu, Z. Gu, X. Deng, and Y. Li, “A novel multi-step reinforcement learning method for solving reward hacking,” *Appl. Intell.*, vol. 49, no. 8, pp. 2874–2888, 2019. [Online]. Available: <https://doi.org/10.1007/s10489-019-01417-4>
- [54] M. Hasanbeig, Y. Kantaros, A. Abate, D. Kroening, G. J. Pappas, and I. Lee, “Reinforcement learning for temporal logic control synthesis with probabilistic satisfaction guarantees,” in *58th IEEE Conference on Decision and Control, CDC 2019, Nice, France, December 11–13, 2019*. IEEE, 2019, pp. 5338–5343. [Online]. Available: <https://doi.org/10.1109/CDC40024.2019.9028919>
- [55] A. K. Bozkurt, Y. Wang, M. M. Zavlanos, and M. Pajic, “Control synthesis from linear temporal logic specifications using model-free

- reinforcement learning,” in *2020 IEEE International Conference on Robotics and Automation, ICRA 2020, Paris, France, May 31 - August 31, 2020*. IEEE, 2020, pp. 10 349–10 355. [Online]. Available: <https://doi.org/10.1109/ICRA40945.2020.9196796>
- [56] M. Cai, M. Hasanbeig, S. Xiao, A. Abate, and Z. Kan, “Modular deep reinforcement learning for continuous motion planning with temporal logic,” *IEEE Robotics Autom. Lett.*, vol. 6, no. 4, pp. 7973–7980, 2021. [Online]. Available: <https://doi.org/10.1109/lra.2021.3101544>
- [57] B. Cui, K. Zhu, S. Li, and X. Yin, “Security-aware reinforcement learning under linear temporal logic specifications,” in *IEEE International Conference on Robotics and Automation, ICRA 2023, London, UK, May 29 - June 2, 2023*. IEEE, 2023, pp. 12 367–12 373. [Online]. Available: <https://doi.org/10.1109/ICRA48891.2023.10160753>
- [58] D. Perrin and J. Pin, *Infinite words - automata, semigroups, logic and games*, ser. Pure and applied mathematics series. Elsevier Morgan Kaufmann, 2004, vol. 141.
- [59] X. Li, C. I. Vasile, and C. Belta, “Reinforcement learning with temporal logic rewards,” in *IROS 2017, Vancouver, BC, Canada, September 24-28, 2017*. IEEE, 2017, pp. 3834–3839. [Online]. Available: <https://doi.org/10.1109/IROS.2017.8206234>
- [60] K. C. Kalagarla, R. Jain, and P. Nuzzo, “Model-free reinforcement learning for optimal control of markov decision processes under signal temporal logic specifications,” in *2021 60th IEEE Conference on Decision and Control (CDC), Austin, TX, USA, December 14-17, 2021*. IEEE, 2021, pp. 2252–2257. [Online]. Available: <https://doi.org/10.1109/CDC45484.2021.9683444>
- [61] O. Maler and D. Nickovic, “Monitoring temporal properties of continuous signals,” in *Formal Techniques, Modelling and Analysis of Timed and Fault-Tolerant Systems, Joint International Conferences on Formal Modelling and Analysis of Timed Systems, FORMATS 2004 and Formal Techniques in Real-Time and Fault-Tolerant Systems, FTRTFT 2004, Grenoble, France, September 22-24, 2004, Proceedings*, ser. Lecture Notes in Computer Science, Y. Lakhnech and S. Yovine, Eds., vol. 3253. Springer, 2004, pp. 152–166. [Online]. Available: https://doi.org/10.1007/978-3-540-30206-3_12